

Preparation, characterization and optical properties of α -Fe₂O₃ films by sol-spinning process

PRATIMA CHAUHAN, S ANNAPOORNI* and S K TRIKHA

Department of Physics and Astrophysics, University of Delhi, Delhi 110 007, India

MS received 19 May 1998; revised 19 July 1998

Abstract. α -Fe₂O₃ films were prepared by sol-spinning process using ferric nitrate as a precursor and 2-methoxy ethanol as the solvent. The films were grown on various substrates by spin coating and were subjected to different annealing temperatures. These were characterized using X-ray and fourier transform infrared spectroscopy (FTIR). The films showed crystallinity at about 500°C. The surface morphology of these films was studied using scanning electron microscopy (SEM) which revealed cracks for films having thickness of the order of 2 μ m. The band gap of these films was observed to be 2.1 eV from UV-vis spectroscopy.

Keywords. Sol-spinning; precursor; nanocrystalline.

1. Introduction

It is a well known fact that iron-oxide occurs in three different forms viz. FeO, Fe₂O₃ and Fe₃O₄. Fe₂O₃ has two phases: α -Fe₂O₃ and γ -Fe₂O₃ (Smart 1963; Feng *et al* 1972; Hattori *et al* 1979; Nakatani and Matsuoka 1983). Fe₂O₃ is a suitable material for gas sensors, photoelectrodes and humidity sensors in α -phase (Chung and Lee 1991; Hu *et al* 1992) and is very weakly ferromagnetic whereas γ -phase is ferromagnetic and is used for magneto-optic recording (Borrelli *et al* 1972). Fe₃O₄ which is ferrimagnetic is used for magnetic recording application (Langet *et al* 1986). Both the γ -Fe₂O₃ and Fe₃O₄ have spinel crystal structure. α -Fe₂O₃ has corundum structure where the oxide ions form a hexagonally close packed array with Fe^{III} ions occupying the octahedral interstices. Conversion from one form to the other is possible by way of oxidation or reduction mechanism. For example, γ -Fe₂O₃ can be obtained from α -Fe₂O₃ by reducing in hydrogen atmosphere and then oxidizing. Recently, we have found a complete conversion of haematite to magnetite by using high energy argon ion irradiation from a dense plasma focus (DPF) (Agarwala *et al* 1997).

Fabrication of iron oxide thin films has been reported primarily using techniques such as sputtering (Chin *et al* 1988), spray pyrolysis (Chang *et al* 1992), metal-organic chemical vapour deposition (MOCVD) (Dhara *et al* 1992) and metal-organic deposition (MOD) (Xue *et al* 1994). Sol-gel processing is a chemical technique which is gaining interest in the area of processing of thin films

and has been employed for preparing iron oxide and substituted iron oxide films (Agarwala *et al* 1997; Takahashi *et al* 1989; Surig *et al* 1993). Among the advantages of sol-spinning process are good composition control and homogeneity, low processing temperature and low cost. In this process, independent control over material can be achieved.

In this paper we report the preparation, structural characterization and optical properties of iron oxide films prepared using 2-methoxy ethanol and iron nitrate.

2. Experimental

Thin films of α -Fe₂O₃ were fabricated using iron(III) nitrate (Fe(NO₃)₃·9H₂O) as precursor and 2-methoxy ethanol as solvent. In this reaction, iron atoms interact with oxygen atoms during hydrolysis, polymerization, condensation and sintering processes, to make the iron atoms bond to each other via oxygen atoms. The gel solution was synthesized by constantly stirring the solution at 50°C in a nitrogen gas flow. Dust and other suspended impurities were removed from the solution by filtering through a 0.2 μ m syringe filter. The viscosity of the solution was controlled by varying the 2-methoxy ethanol content and solvent to solute ratio was standardized to yield good spin coated films by trial. The precursor films were coated on various substrates by spin coating the above solution at a speed of about 3000 rpm. The substrates used include fused quartz and single crystal silicon wafers grown along [111]. The spin cast films were heated in air at 350°C for evaporation of the solvent. Multilayered films were grown by successive coatings of the solution. After each coating the drying

*Author for correspondence

process was repeated to ensure complete removal of the volatile matter. Films of different thicknesses (depending upon the number of layers coated) were obtained by this method and the thicknesses were estimated using a Dektak thin film analyser to an accuracy of $\pm 10 \text{ \AA}$.

The crystal structure of the films was examined by X-ray diffraction using a Rigaku Rotaflex diffractometer using a Cu-K α radiation ($\lambda = 1.5918 \text{ \AA}$) at 40 KeV. The fourier transform infrared spectroscopy (FTIR) was performed using a Nicolet 510 P FTIR spectrophotometer.

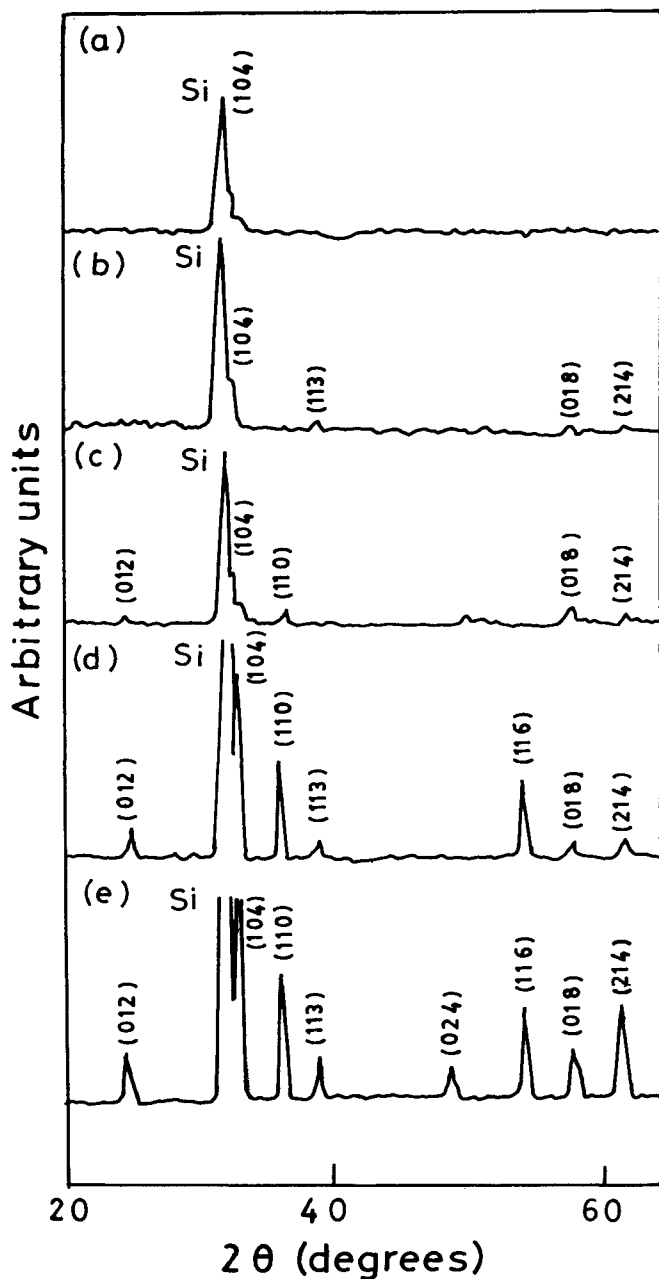


Figure 1. X-ray diffraction patterns of $\alpha\text{-Fe}_2\text{O}_3$ on silicon substrate: (a) as grown, (b) annealed at 400°C , (c) annealed at 500°C , (d) annealed at 600°C and (e) annealed at 700°C .

The surface morphology was analysed by a JEOL JSM-840 scanning electron microscope (SEM). The optical properties were analysed using a Shimadzu model 160-A spectrophotometer in the wavelength range 200–1100 nm.

3. Results and discussion

3.1 X-ray diffraction

XRD patterns of the films were obtained on single crystal silicon substrates. Figures 1a, b, c, d, and e give the XRD patterns of the as grown film and films annealed at 400°C , 500°C , 600°C and 700°C for 3 h, respectively. Figure 1a shows the nanocrystalline structure of the as grown film indicated by a slight hump in the (104) peak. For the films annealed at 400°C the diffraction peaks start appearing and become prominent as the annealing temperature increases. All the films grown on silicon substrates and annealed above 400°C for 3 h are polycrystalline and belong to hexagonal α -phase. The lattice constants of the films were obtained from the diffraction peaks and were found to be $a = 4.983 \pm 0.001 \text{ \AA}$, $c = 13.765 \pm 0.001 \text{ \AA}$, which are in good agreement with the values obtained from ASTM data card for $\alpha\text{-Fe}_2\text{O}_3$ powder.

Grain size of the films was calculated by using Scherrer's equation (Klug and Alexander 1974)

$$D = k\lambda/(\beta \cos \theta), \quad (1)$$

where D is the grain size, λ the X-ray wavelength, β (in radians) is the full width at half maxima (FWHM) of the peaks, θ the reflection angle and k is a constant approximately equal to unity. Table 1 shows the calculated grain size for the annealed films. From table 1 we notice that D increases with annealing temperature. The small grain size (nano crystallites) corresponding to annealing temperatures 400°C and 500°C clearly indicates that the crystallization has just set in and it is also evident from the small peaks observed in diffraction pattern as shown in figures 1b and 1c, respectively.

3.2 Scanning electron microscopy

Surface morphology of the films was studied using scanning electron microscope. SEM photographs of

Table 1. Estimated grain size from XRD data for different annealing temperatures.

Temperature ($^\circ\text{C}$)	2θ (deg)	FWHM (radians)	D (nm)
400	32.64	6.02×10^{-3}	26.66
500	32.84	5.50×10^{-3}	29.21
600	33.24	3.67×10^{-3}	43.86
700	33.66	1.83×10^{-3}	87.82

0.5 μm thick films as grown and annealed at 700°C are shown in figures 2a and b. Both the photographs reveal the surface to be fairly smooth with no cracks and pin holes. We have studied the effect of thickness ($>0.5 \mu\text{m}$)

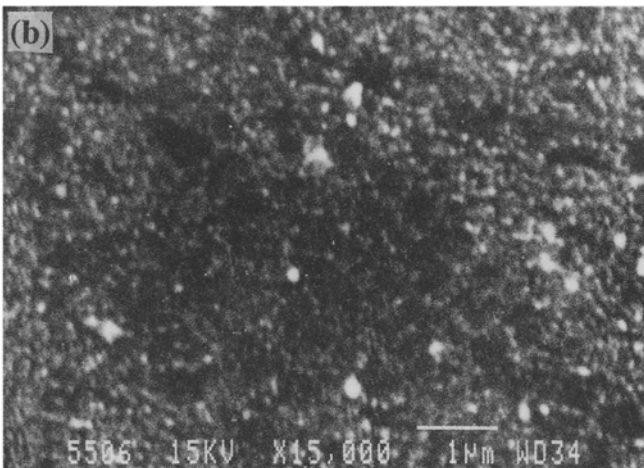
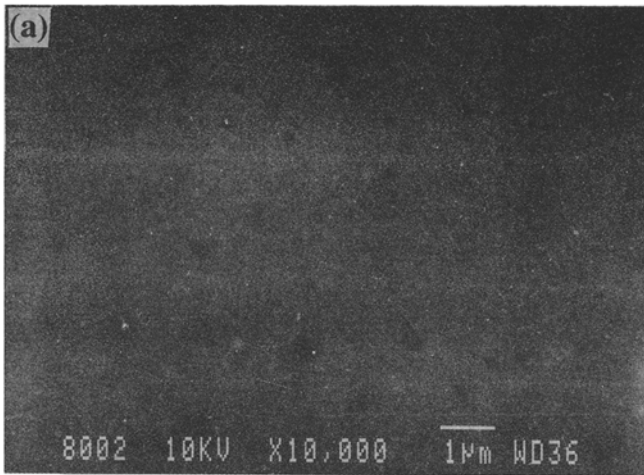


Figure 2. SEM micrographs of 0.5 μm α -Fe₂O₃ films on silicon substrate: (a) as grown and (b) annealed at 700°C.

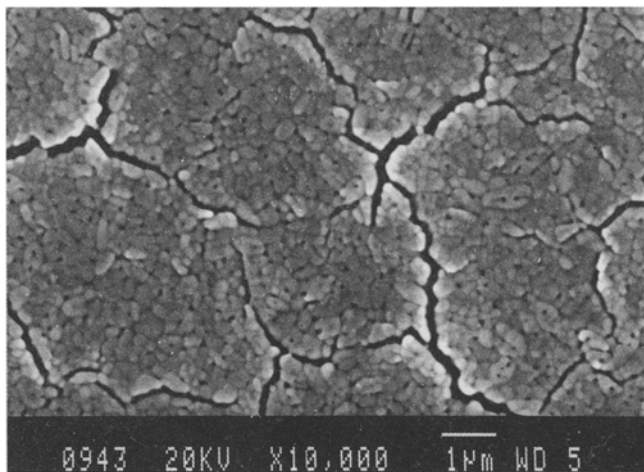


Figure 3. SEM micrograph of 2 μm α -Fe₂O₃ film annealed at 700°C on silicon substrate.

on the surface morphology. The surface morphology of 2 μm thick film annealed at 700°C is shown in figure 3. The grain size is found to increase with increasing film thickness as is evident from the micrographs. Further we notice nanocracks develop in the films of thickness $\sim 2 \mu\text{m}$. As the film thickness increases, bulk diffusion tends to increase. Consequently, small grains tend to coalesce to form larger grains. The possible cause of development of cracks may be due to thermal mismatch between the substrate and the film. Undoubtedly, the grain size as well as the appropriate thickness of the film are the important parameters in the fabrication of devices which have been discussed by earlier workers (Chung and Lee 1991; Dhara *et al* 1992).

3.3 Fourier transform infrared spectroscopy

Figures 4a and b show the FTIR spectra of films on silicon substrate obtained from reflection mode. Blank silicon substrates thermally processed simultaneously with the samples were used as background. As grown films (refer to curve (a)) show a broad absorption band around 530 cm^{-1} which is characteristic of α -Fe₂O₃ films. However, for films annealed at 700°C (refer to 4b), a sharp peak at 1085 cm^{-1} appears, which may be assigned to crystalline Fe–O modes. This peak is useful in monitoring the amorphous to crystalline phase transition of α -Fe₂O₃ films (Xue *et al* 1994).

3.4 Ultraviolet-visible spectroscopy

The optical quality of the films was investigated using films grown on quartz substrates from the transmission spectra in the wavelength range 400–1100 nm. The spectral transmittance of as grown films of thickness 0.5 μm and films annealed at 700°C are shown in

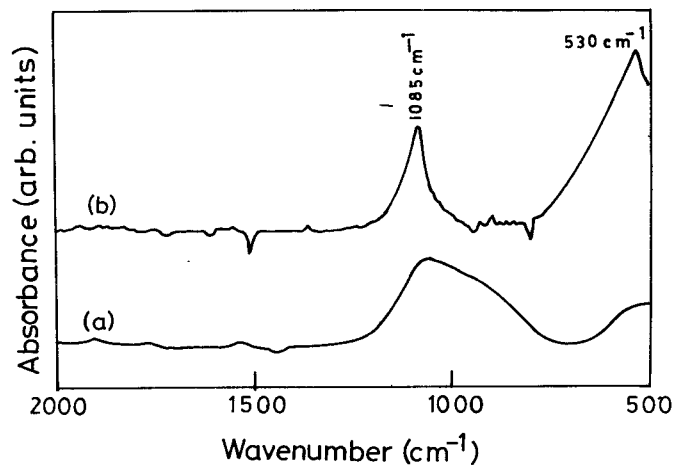


Figure 4. FTIR absorption spectra of α -Fe₂O₃ films on silicon substrate for (a) as grown and (b) annealed at 700°C.

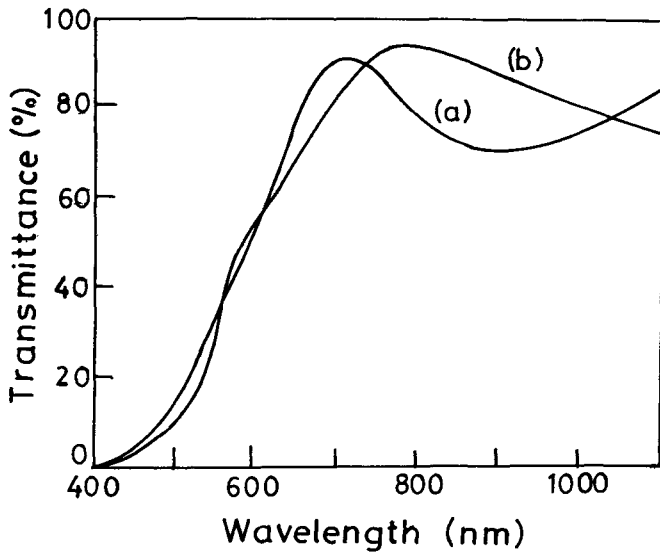


Figure 5. UV-vis transmission spectra of 0.5 μm thick film: (a) as grown and (b) annealed at 700°C on quartz substrate.

figure 5. The optical transmittance was found to be $>90\%$ in the scanned wavelength range. Further, we notice that the absorption wavelength (λ_c) shifts to longer wavelength side with increasing annealing temperature. The shift of λ_c results in a change in apparent colour of the film. Further the shift of λ_c with annealing may be explained due to the formation of crystalline $\alpha\text{-Fe}_2\text{O}_3$ along with the removal of carbon.

Figure 6 shows a graph between the transmittance of the film annealed at 700°C as a function of thickness corresponding to $\lambda = 400\text{ nm}$. It shows that for thin films the transmission is linearly dependent on thickness and for thickness $> 1.5\ \mu\text{m}$ there is a departure from linearity. It has been observed from SEM micrographs that films of thickness $> 1.5\ \mu\text{m}$ develop cracks. This could be one of the major causes of the observed deviation from linearity.

The transmittance of the films exhibited a sharp absorption edge at 0.5 μm characteristic of inter-band transitions. The band-to-band transitions are described by the relation (Koffyberg *et al* 1979)

$$\alpha(\nu) = A(h\nu - E_g)^n, \quad (2)$$

where $\alpha(\nu)$ is the absorption coefficient, A a constant, n depends on the nature of optical transition, $h\nu$ the photon energy, and E_g is the band gap. The absorption coefficient in the fundamental absorption region was determined from the transmission spectra as a function of frequency, ν using the relation:

$$\alpha(\nu) = (1/t) \ln(1/T), \quad (3)$$

where t is the film thickness and T the transmittance

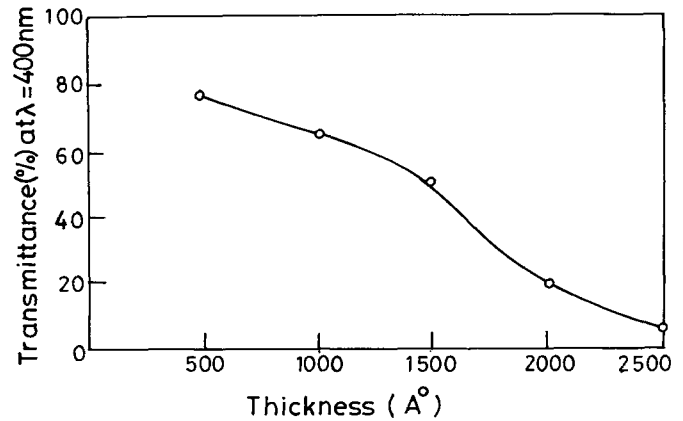


Figure 6. Transmittance % at $\lambda = 400\text{ nm}$ vs thickness of $\alpha\text{-Fe}_2\text{O}_3$ films.

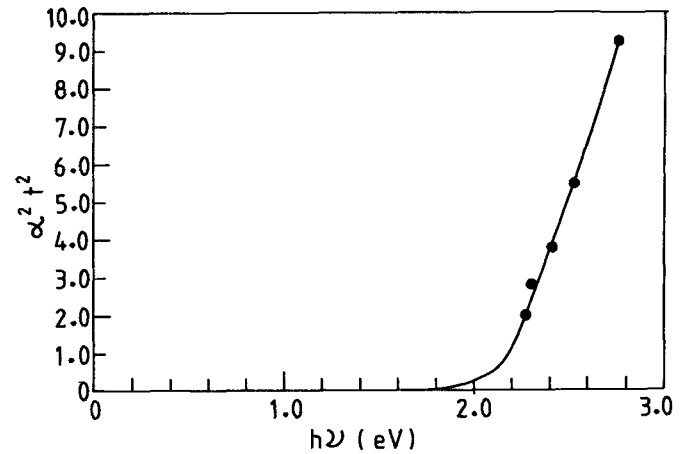


Figure 7. Plot of α^2 vs $h\nu$ for film annealed at 700°C.

of the film. For $\alpha\text{-Fe}_2\text{O}_3$ thin films, the best linear graph (α vs $h\nu$) was obtained for $n = (1/2)$, as shown in figure 7 corresponding to the direct allowed transition. In the high energy region of absorption edge, α^2 vs $h\nu$ plot was taken as the prime evidence for a direct band gap. The intercept of the straight line on the $h\nu$ axis gives the band gap. The optical band gap for $\alpha\text{-Fe}_2\text{O}_3$ thin film was found to be 2.1 eV. The band gap obtained is in agreement with the earlier reports on $\alpha\text{-Fe}_2\text{O}_3$ films prepared by other methods (Kennedy and Frewe 1978; Themburkar 1996).

4. Conclusions

The $\alpha\text{-Fe}_2\text{O}_3$ films were prepared using iron nitrate and 2-methoxy-ethanol using sol-spinning technique. Uniform and homogenous films were obtained on silicon and quartz substrates. The as grown films were nanocrystalline

and grain size increased on annealing. Grain size was found to increase with increasing thickness of the films also. However, thin films (~0.5 μ m) were uniform with no cracks and pin holes. Cracks develop as the thickness increases beyond 1.5 μ m. These spin coated films of thickness ~0.5 μ m were found to be highly transparent and therefore may find its use in magneto-optical applications.

Acknowledgements

The authors wish to thank Dr N C Mehra and Dr S K Shukla, University Science and Instrumentation Centre (USIC), University of Delhi, Delhi, for their kind help in carrying out the X-ray and SEM studies. We also wish to thank Dr B D Malhotra, National Physical Laboratory, New Delhi, for extending FTIR and UV spectrophotometer. One of the authors (PC) wishes to thank the University Grants Commission (UGC), New Delhi, for providing a fellowship.

References

- Agarwala P, Annapoorni S, Srivastava M P, Rawat R S and Chauhan P 1997 *Phys. Lett.* **A231** 434
- Borrelli N F, Chen S L and Murphy J A 1972 *IEEE Trans. Mag.* **MAG-8** 648
- Chang W D, Deng M C, Tsai T and Chin T S 1992 *Jpn J. Appl. Phys.* **31** 1334
- Chin M M, Kakalec M A, Ju K, Tsang C and Castaillo G 1988 *Jpn J. Appl. Phys.* **24** 2988
- Chung W Y and Lee D D 1991 *Thin Solid Films* **200** 329
- Dhara S, Kotnala R K and Rastogi A C 1992 *Jpn J. Appl. Phys.* **31** 3853
- Feng J S Y, Bajorek C H and Nicolet M A 1972 *IEEE Trans. Mag.* **MAG-8** 277
- Hattori S, Ishii Y, Shinohara M and Nakagawa T 1979 *IEEE Trans. Mag.* **MAG-15** 1549
- Hu L L, Yoko T, Kozuka H and Sakka S 1992 *Thin Solid Films* **219** 18
- Kennedy J H and Frewe Karl W 1978 *J. Electrochem. Soc.* **125** 2371
- Klug H P and Alexander L E 1974 *X-ray diffraction procedures* (New York: Wiley) 2nd ed.
- Koffyberg F P, Dwight K and Wold A 1979 *Solid State Commun.* **30** 433
- Langet M, Labeau M, Bochu B and Joubert J C 1986 *IEEE Trans. Mag.* **MAG-22** 151
- Nakatani Y and Matsuoka M 1983 *Jpn J. Appl. Phys.* **22** 233
- Smart J S 1963 *Magnetism* (eds) G T Rado and H Suhl (New York: Academic Press)
- Surig C, Hempel K A and Bonnenberg D 1993 *Appl. Phys. Lett.* **63** 2836
- Takahashi N, Kakuda N, Veno A, Yamaguchi K and Fuji T 1989 *Jpn J. Appl. Phys.* **28** L244
- Thembhurkar Y D 1996 *Bull. Mater. Sci.* **19** 155
- Xue S, Qusi Benomar W and Lessard R A 1994 *Thin Solid Films* **250** 194